Journal of Alloys and Compounds 527 (2012) 240–246

Contents lists available at SciVerse ScienceDirect

Journal of Alloys and Compounds

journal homepage: www.elsevier.com/locate/jallcom

# Effect of high magnetic field on alloy carbide precipitation in an Fe–C–Mo alloy

T.P. Hou, Y. Li, K.M. Wu*

*International Research Institute for Steel Technology, Wuhan University of Science and Technology, Wuhan 430081, China*

ARTICLE INFO

*Article history:*
Received 19 November 2011
Received in revised form 22 February 2012
Accepted 24 February 2012
Available online xxx

*Keywords:*
Alloys
Phase transitions
Precipitation
High magnetic fields
Transmission electron microscopy

ABSTRACT

The effect of a 12-T high magnetic field on molybdenum carbide precipitation during isothermal transformation in an Fe–C–Mo alloy was investigated. Three kinds of alloy carbides ($M_2C$, $M_3C$ and $M_6C$) were precipitated when specimens were treated both with and without a 12-T magnetic field. The precipitation of $(Fe,Mo)_6C$ started from the early stage under the high magnetic field, whereas it happened late during conventional treatment. The observed results suggested that the precipitation of $(Fe,Mo)_6C$ was remarkably promoted when specimens were treated in a 12-T magnetic field. In the meantime, the concentration of substitutional solute atoms Fe and Mo in the carbide of $(Fe,Mo)_6C$ was greatly influenced by a strong magnetic field. The promotion of specific alloy carbide and the substitutional solute atom concentration change in alloy carbides were attributed to their magnetization differences, which resulted in the change of Gibbs magnetic free energy of the alloy carbides. The investigation of alloy carbide precipitation under high magnetic fields could contribute to a better understanding of phase transformation of alloy carbides and to the heat-treatment and fabrication of high-strength energy materials.



## 1. Introduction

Metal carbides play an important role in the development of structural steels, for example, in the strengthening and toughening of microalloyed steels and in the exploitation of secondary hardened steels for service at elevated temperatures. Molybdenum carbides can be introduced into the steel as hydrogen trapping sites to enhance the resistance to static fracture of components such as springs, bolts and power plant structural parts [1]. Mo-containing low alloy steels are often used in important structural applications due to good mechanical properties at elevated temperatures and prolonged service time, as in the petrochemical and energy industries. Owing to the scientific and industrial importance, Fe–C–Mo alloy system has attracted much research interest. A deep "bay" at intermediate temperature in the TTT diagram and the peculiar morphology of transformation product (degenerate ferrite) in and below the "bay region" [2–8] during isothermal transformation are well understood. Many studies on Mo, W and Cr carbide precipitation have been carried out [9–12]. Some of these studies focus on carbide precipitation during isothermal transformation without applying a magnetic field [3] and others are concentrated on cementite precipitation from martensite during tempering in a high magnetic field [13,14]. Although some progress has been made, the effects of magnetic field on alloy carbide formation need further study. Insights into these aspects would contribute to a better understanding of alloy carbide precipitation behavior in a high magnetic field.

In recent years, the effects of strong magnetic fields on various phase transformations in steels, including martensite [15,16], bainite [17,18], ferrite [19,20] and pearlite [21] transformations have attracted much research interest. It is usually considered that strong magnetic field has a significant influence on ferromagnetic materials. However, not only the difference of magnetic moment but also magnetocrystalline anistropy, shape magnetic anisotropy, induced magnetic anisotropy and magnetostriction can affect the nucleation and growth rates, transformation kinetics, variants and microstructure of product phases [13,22]. Liu et al. [23] reported that the magnetization and Curie temperature increase with increasing external magnetic field strength in α-Fe, Fe-C and Fe-Mo systems. Molybdenum carbides are iron carbides with a proportion of substitutional solute atoms of Fe replaced by Mo [9]. It is therefore expected that the precipitation of molybdenum carbides can be influenced by strong magnetic fields, to which, however, less attention is paid. The aim of the present study is to investigate the effects of a 12-T magnetic field on molybdenum carbide precipitation during isothermal transformation from austenite-to-degenerate ferrite (bainite) of an Fe–C–Mo alloy.

* Corresponding author. Tel.: +86 27 68862772; fax: +86 27 68862807.
*E-mail addresses:* wukaiming@wust.edu.cn, wukaiming2000@yahoo.com (K.M. Wu).

0925-8388/$ – see front matter © 2012 Elsevier B.V. All rights reserved.
doi:10.1016/j.jallcom.2012.02.153

**Table 1**
Chemical composition of the investigated steel (wt.%).

| C | Si | Mn | P | S | Mo | Fe |
|---|---|---|---|---|---|---|
| 0.28 | <0.004 | <0.001 | <0.003 | <0.004 | 3.0 | Bal. |

## 2. Experimental

In order to avoid the complication of interactive effects among multiple solutes, the alloy studied was prepared by vacuum induction melting utilizing high purity electrolytic iron, graphite and molybdenum. The chemical composition is shown in Table 1. Ingots were hot-rolled and then homogenized at 1250 °C for two days in a vacuum quartz capsule. Specimens of 4 mm × 4 mm × 18 mm were cut from the homogenized sample and austenitized at 915 °C for 10 min in an argon atmosphere and then isothermally transformed in a salt bath at 530 °C with and without applying a 12-T magnetic field. Specimens were immediately quenched after isothermal holding. After heat treatment specimens were polished and etched with 3 vol% nital solution for microscopic analysis.

Two types of specimens were examined by means of transmission electron microscopy (TEM): thin foils and gold extraction replicas. Thin foil observation is crucial to determine the orientation relationship between the precipitate and the matrix. The foils were sliced from bulk specimens, mechanically ground to about 50 μm in thickness. These specimens were twin-jet electropolished at a voltage of 40 V. The electrolyte consisted of 10 vol% perchloric acid and 90 vol% glacial acetic acid. For phase identifications, thin foils were examined by TEM using the JEM 2010 HT microscope.

Regarding the measurements of the concentration of substitutional solute atoms Fe and Mo in carbides, Au replica specimens, were prepared in order to avoid the influence of the matrix on the measured concentrations. The specimens were deeply etched with a nital solution (4 vol%) for a few seconds. An Au coating of 20–30 nm was deposited onto the etched surface in a vacuum system. The gold film was then cut with a sharp blade to divide it into several smaller squares (~1 $mm^2$). Then, chemical etching in a nital solution (8 vol%) was conducted to remove the gold film with the extracted carbides. Then the gold film was washed in methanol and floated off in distilled water in order to make the film flattened. Finally, these films were mounted on copper grids for TEM analysis. The concentration of isolated $M_6C$ particles was measured using a JEM2100F TEM equipped with an energy-dispersive spectroscopy (EDS) system. Totally 85 isolated carbides from the specimens isothermally treated at 530 °C for 3600 s with and without the magnetic field were examined. A photograph was taken for each individual particle analyzed in order to correlate the particle size with composition. Care was taken to ensure that unbiased distributions of particle sizes were studied.

## 3. Results

### 3.1. Identification of $M_6C$ alloy carbides

The carbides precipitated in the specimen isothermally treated at 530 °C for 600 s in a 12-T magnetic field are shown in Fig. 1. The carbide pointed by the arrow in the figure is considered to be $(Fe,Mo)_6C$ on the basis of EDS analysis. In order to minimize error in analyzing the composition of carbides, analyses were carried out only on the carbides which overhung from the foils. In the meantime, selected area electronic diffractions (SAED) of carbides were carried out to further identify the carbides. Fig. 2 shows the bright and dark field images, SAED patterns and the indexation of $M_6C$ carbide in the specimen isothermally transformed at 530 °C for 3600 s in a 12-T magnetic field. In this figure, the matrix is ferrite which belongs to b.c.c. and the crystal structure of $M_6C$ is f.c.c. [10]. Fig. 2 demonstrates that the spheroidal type of carbide is $M_6C$, which is precipitated from ferrite matrix. Fig. 3 shows the bright and dark field images of a rod-like type of carbide in the specimen isothermally transformed at 530 °C for 3600 s in a 12-T magnetic field. Similarly, this type of carbide was confirmed to be $M_6C$.

### 3.2. Nucleation sites of $M_6C$ alloy carbides

Fig. 4 shows the nucleation sites of molybdenum carbides in the specimens treated in 12-T magnetic field. It is seen in Fig. 4 that the $M_6C$ carbide (marked by a long thin arrow) is evidently formed at the interphase boundary. It is also found that the $M_6C$ carbide

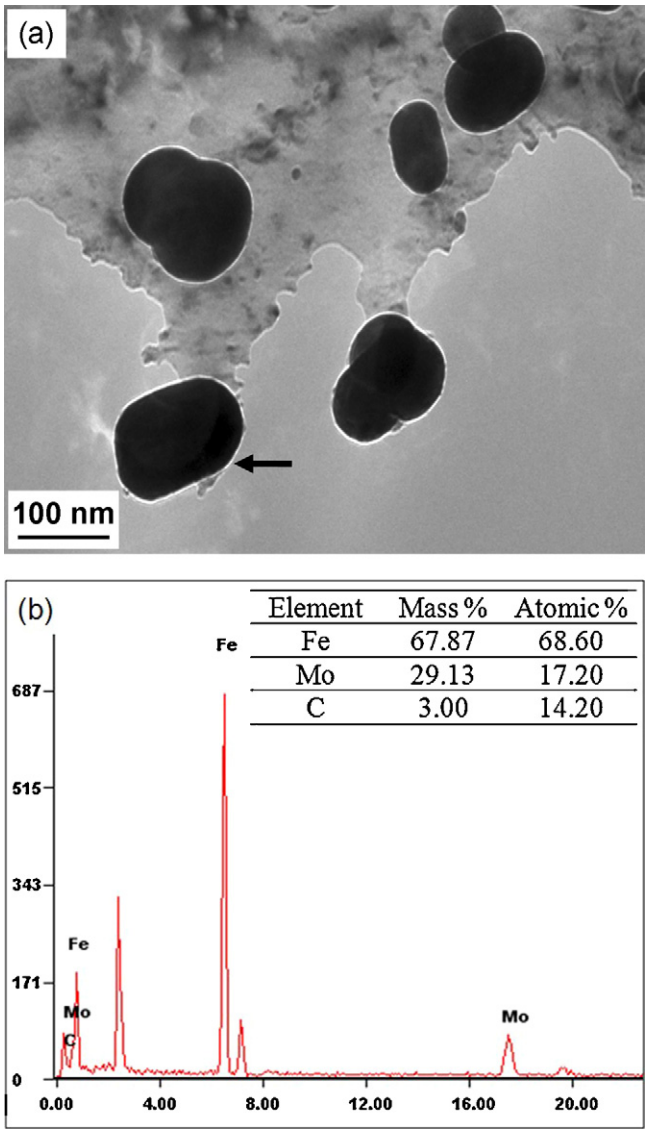


**Fig. 1.** Morphology and the EDS analysis of $M_6C$ carbide (arrowed) in the specimen isothermally transformed at 530 °C for 3600 s when a 12-T magnetic field was applied.

(marked by a short thick arrow) is formed at the dislocations within the ferrite matrix.

### 3.3. Morphology and size of alloy carbides

The different kinds of morphology of carbides precipitated in the present alloy are illustrated in Fig. 5. $M_2C$ without the magnetic field is a lath-like or needle-like particle (Fig. 5a). It is usually 100–150 nm long and approximately 10 nm thick. $M_3C$ (including $Fe_3C$) is 100–200 nm in length and 10–30 nm in thickness with the conventional heat treatment in Fig. 5b. It is usually appeared to be of an equiaxed or irregular shape depending on its orientation with the observed plane. The $M_2C$ type of carbide was identified to be $(Fe,Mo)_2C$ and the $M_3C$ type $(Fe,Mo)_3C$ according to the diffraction and EDS analyses. Most of $M_6C$ carbides are spheroidal in shape, usually 50–100 nm in diameter (Fig. 5c). Some of them have a rod-like shape, being approximately 50–100 nm in length and 50~80 nm in width (Fig. 5c). These two kinds of morphology for $M_6C$ carbide have also been reported by Davenport and Honeycombe [24] and Shtansky and Inden [9].

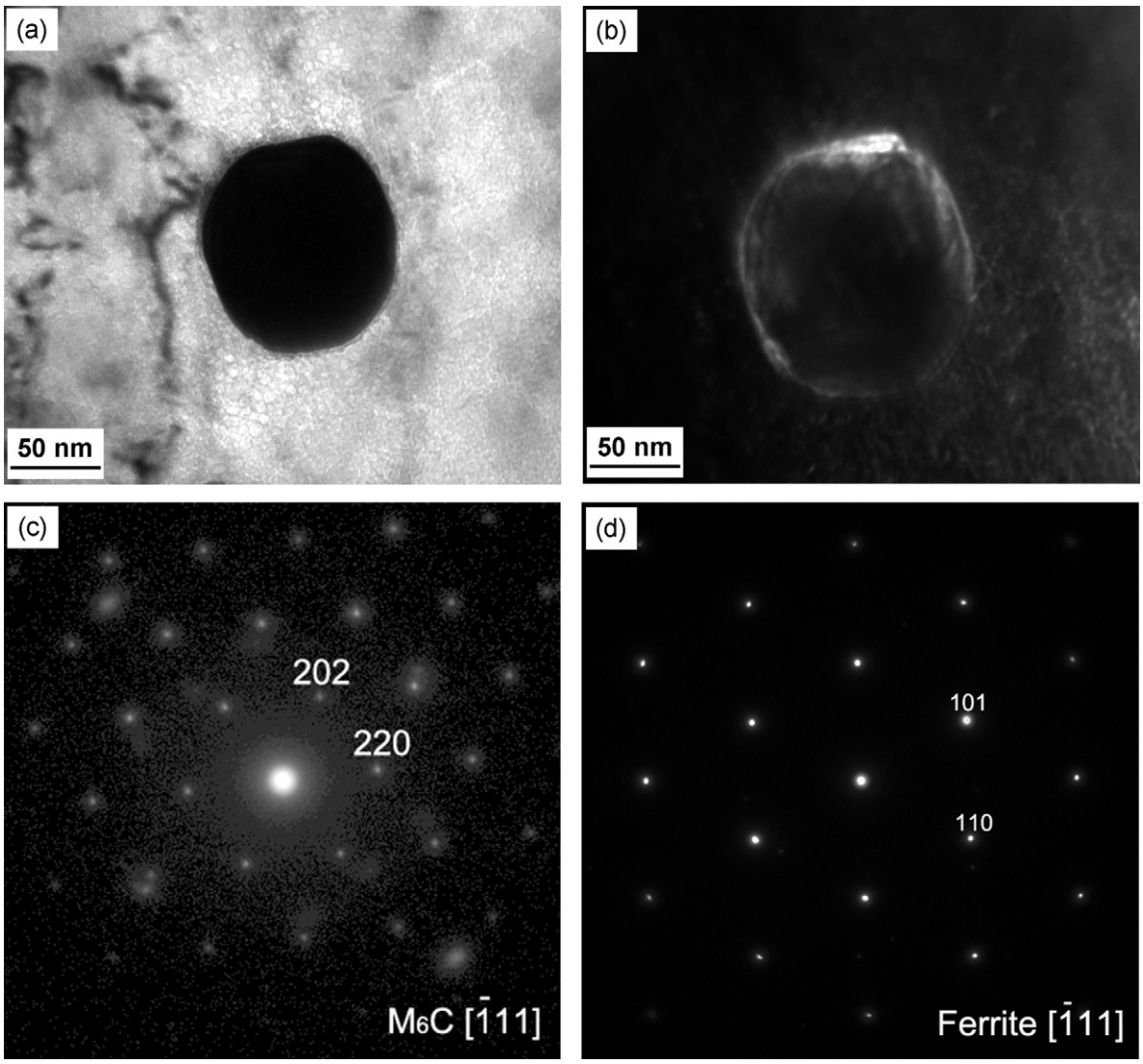


**Fig. 2.** Morphology, SAED patterns and the interpretation of a spherical type of $M_6C$ in the specimen isothermally transformed at 530 °C for 3600 s when a 12-T magnetic field was applied: (a) bright field, (b) dark field, (c) SAED pattern of $M_6C$ and (d) SAED pattern of ferrite matrix.

### 3.4. Sequence of alloy carbide precipitation

Fig. 6 shows TEM observations of carbides in the specimens isothermally treated at 530 °C for a longer holding time (3600 s) without (Fig. 6a) and with (Fig. 6b) the presence of a 12-T magnetic field. The spheroidal particles in Fig. 6a and b are $M_6C$ type carbides. The carbides precipitated at 530 °C are summarized in Table 2 for the specimens treated without and with the magnetic field. When the magnetic field was not present, $M_2C$ and $M_3C$ were precipitated at earlier transformation stage and $M_6C$ was precipitated at later transformation stage; in contrast, when a 12-T magnetic field was present, $M_6C$ was precipitated at all the transformation stages.

### 3.5. Measured concentration of substitutional solute atoms in the carbide of $M_6C$

In the present work, the same type of carbide $M_6C$ was both precipitated during the longer holding time (3600 s) in both specimens heat treated with and without magnetic field (Table 2). For comparison, the concentration of substitutional solute atoms of Fe and Mo in the carbide of $M_6C$ was measured to investigate substitutional solute concentration change. The measured concentration of substitutional solute atoms in the carbide of $M_6C$ is listed in Table 3. It is seen that the concentration of Fe atom in the carbide was remarkably increased whereas the concentration of Mo atom was decreased when the specimen was isothermally held at

**Table 2**
The precipitation of molybdenum carbides in the specimens isothermally treated 530 °C without and with a 12-T magnetic field.

| | Without a 12-T magnetic field | | With a 12-T magnetic field | |
|---|---|---|---|---|
| Time | 1000 s | 3600 s | 600 s | 3600 s |
| Type | $M_2C$ $M_3C$ | $M_6C$ | $M_6C$ | $M_6C$ |
| Carbide | $(Fe,Mo)_2C$ $(Fe,Mo)_3C$ | $(Fe,Mo)_6C$ | $(Fe,Mo)_6C$ | $(Fe,Mo)_6C$ |

**Table 3**
The concentration of Fe and Mo atoms in the carbide of $M_6C$ with and without the presence of high magnetic field isothermally treated at 530 °C for 3600 s.

| Magnetic field OFF | | | | Magnetic field ON | | | |
|---|---|---|---|---|---|---|---|
| Fe (wt.%) | | Mo (wt.%) | | Fe (wt.%) | | Mo (wt.%) | |
| Average | Standard deviation ($\sigma$) | Average | Standard deviation ($\sigma$) | Average | Standard deviation ($\sigma$) | Average | Standard deviation ($\sigma$) |
| 38.69 | 0.98 | 61.30 | 0.98 | 67.16 | 4.48 | 32.78 | 4.48 |

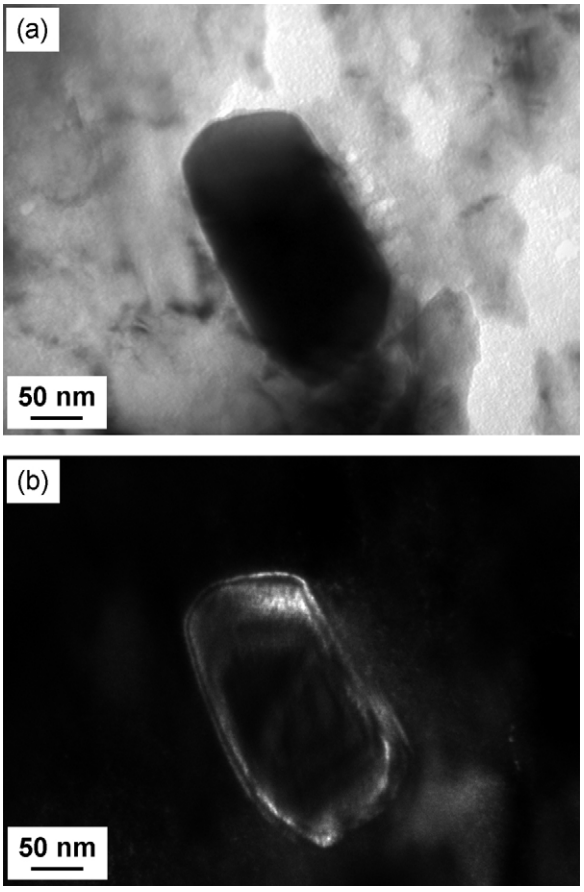


**Fig. 3.** TEM bright field and dark field images of a rod-like type of $M_6C$ in the specimen isothermally transformed at 530 °C for 3600 s when a 12-T magnetic field was applied.

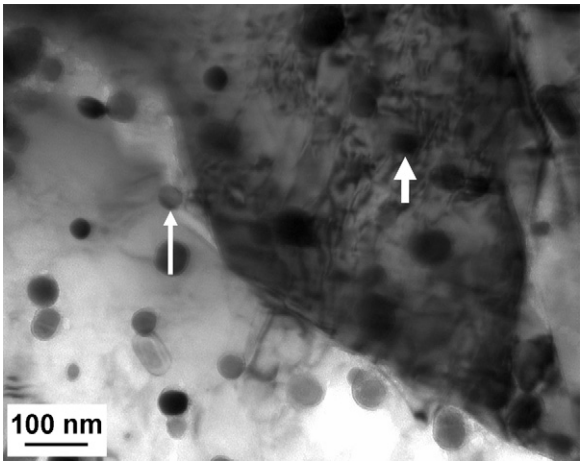


**Fig. 4.** Nucleation sites of alloy carbides in the specimens isothermally transformed at 530 °C for 3600 s when a 12-T magnetic field was applied.

530 °C under the 12-T magnetic field. The average atomic ratio of Fe/Mo is 1.08 and is in good agreement with the formula of carbide $Fe_3Mo_3C$ when the specimen was isothermally held at 530 °C for 3600 s without the presence of magnetic field whereas it changed into 3.91 with the presence of magnetic field. It can be seen that atomic ratio of Fe/Mo was greatly increased by the application of strong magnetic field. The concentration of Mo atom in the carbide of $M_6C$ (Table 3) precipitated in the specimen tempered for a longer time (3600 s) with the presence of magnetic field is much lower than that in the literatures (Table 4) treated with traditional heat treatment. It means that the high magnetic field reduces the concentration of Mo atom in alloy carbides.

## 4. Discussion

### 4.1. Molybdenum carbides and stability

Phase relationships in Fe–C–Mo system have been of great interest because of the importance of molybdenum as an alloying element in steels. An extensive study on the equilibrium of the Fe–C–Mo system was first reported by Takei [28]. In that work, only two carbide phases were found. Five kinds of carbides were later identified in molybdenum steels [25]. It is reported that the steel composition has a significant influence on the precipitation of carbides [9]. Thus different kinds of carbides exist depending upon the composition of steels. In the present work, $M_2C$, $M_3C$ and $M_6C$ were detected at a low austenitizing temperature (915 °C) and an intermediate transformation temperature.

The $M_{23}C_6$ carbide and MC carbide were not observed in the specimens isothermally treated at the temperature of 530 °C in the present work. This result is in agreement with the experimental results reported in the literature [3], in which the $M_{23}C_6$ carbide and MC carbide do not form during the isothermal transformation from austenite to degenerate ferrite (bainite) in a Fe–0.19%C–2.30%Mo alloy. Shtansky and Inden [9] reported that the $M_{23}C_6$ carbide forms at prior austenite grain boundaries and penetrates into the grains with increasing tempering time. The $M_{23}C_6$ carbide is of irregular shape with an average size in the range of 5–10 μm. It even may reach a size of about 15 μm at longer tempering times [9]. In this study, this kind of carbide was not observed in any specimen. It has been reported that the MC carbide does not form even after long time (3000 h) tempering [9]. The MC carbide was also not observed in the present work. It is thus considered that the $M_{23}C_6$ and MC carbides would not form in the specimens treated under the conditions used in the present study.

Sato et al. [25] classified carbides into three groups according to their stability: (1) stable carbides $M_3C$ and $M_6C$; (2) metastable carbide $M_{23}C_6$; and (3) carbide with intermediate stability $M_2C$. However, there are still disagreements concerning the stability of

**Table 4**
The concentration of Mo (wt.%) atoms in the $M_6C$ carbide in the literatures.

| Magnetic field OFF, Mo (wt.%) | |
|---|---|
| 45–62 (700–900 °C) | Ref. [25] |
| 61.4–63.6 (727 °C) | Ref. [26] |
| 48.15 (874 °C) | Ref. [27] |

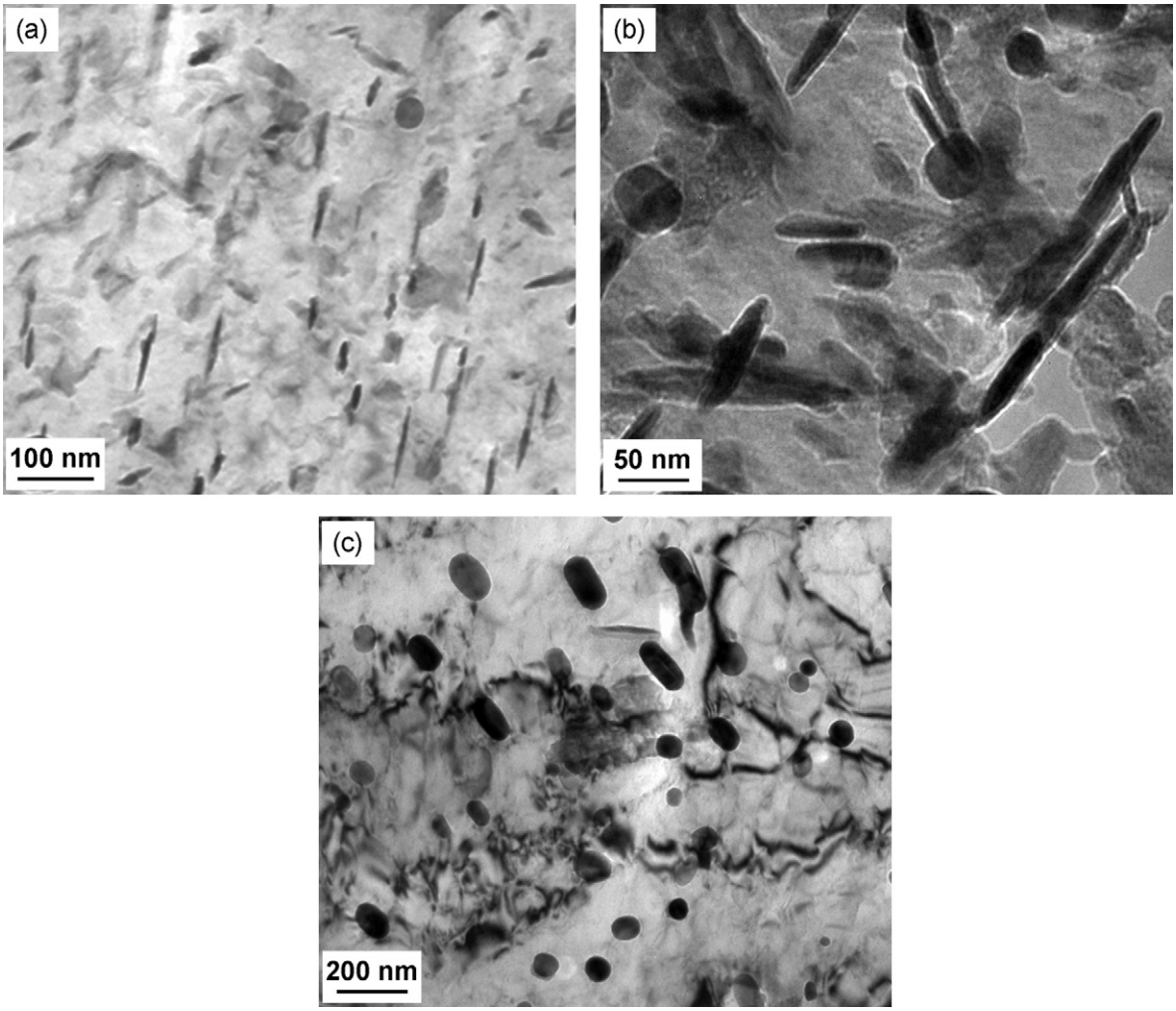


**Fig. 5.** Morphology of precipitated carbides in the present alloy: (a) lath-like $M_2C$ carbides without the magnetic field, (b) spheroidal $M_3C$ carbides without the magnetic field and (c) spheroidal and rod-like $M_6C$ carbides with a 12-T magnetic field.

some of the carbides, such as $M_3C$, $M_{23}C_6$ and $M_2C$ [9]. Shtansky and Inden [9] reported that $M_{23}C_6$ is stable and $Fe_2MoC$ is also stable. However, Uhrenius and Harvig [26] suggested that $M_{23}C_6$ carbide is not stable in the pure Fe–C–Mo system. In the present work, the sequence of carbide precipitation was $M_2C \rightarrow M_3C \rightarrow M_6C$ when no magnetic field was applied at 530 °C [2], whereas $M_2C$ and $M_3C$ did not precipitate, the precipitation of $M_6C$ starts from the early stage when a 12-T magnetic field was applied. This indicates that the stability of different kinds of carbides may be affected by the application of a high external magnetic field. Actually, it has been found that the precipitation sequence of transition iron carbides is changed by strong magnetic field [14,29].

### 4.2. Influence of high magnetic field on the precipitation sequence of carbides

Carbides can be magnetized to some extent in a high magnetic field thus the Gibbs free energy is lowered in relation to their magnetization. The corresponding Gibbs free energy (magnetic free energy $\Delta G^M$) drop amounts to $-\int B_0 \cdot dM$ [30] (where $B_0$ is the induction of the applied magnetic field and $M$ stands for the magnetization). Previous studies have revealed that applied field effectively promoted the precipitation of $\chi$-$Fe_5C_2$ iron carbide [14,29,31], compared to the usual $\varepsilon$-$Fe_2C$ and $\eta$-$Fe_2C$ iron carbides, because the influence of the magnetic field on the Gibbs free energy of $\chi$-$Fe_5C_2$ is the most remarkable. In the present work, the magnetic field has promoted the precipitation of alloy carbide $M_6C$, which is similarly attributed to the reduction of Gibbs free energy by the magnetic field.

The spontaneous and induced magnetization is used by the Weiss molecular field theory [32]. A magnetic field is applied to an ensemble of $N$ atoms; each having a magnetic moment $m$. Magnetic moments are aligned in the direction of applied field in opposition to thermal agitation. The magnetization of this ensemble is expressed as Eq. (1). The internal field induction reads

$$B = B_0 + \lambda M \tag{1}$$

where $B_0$ is the applied field and $\lambda$ is the molecular field constant. $\lambda$ can be obtained by the following equation:

$$T_c = \frac{(j+1)Nn_B^2\mu_B^2\lambda}{3jk} \tag{2}$$

where $j$ is the quantum number associated with the total angular momentum of an atom, which is difficult to be ascertained. In the present work, $j$ is determined to be $j=1$, because $m_{Fe}$ (equal to 2.22 $\mu_B$) with $j=1$ is not only fortuitously close to ferromagnetic state but also suitable to paramagnetic state [33]. $N$ is the number of atoms per unit volume, $n_B$ is the effective Bohr magneton number. $k$ is the Boltzman constant, $T$ is the absolute temperature, $\mu_B$ is the Bohr magneton and $T_c$ is Curie

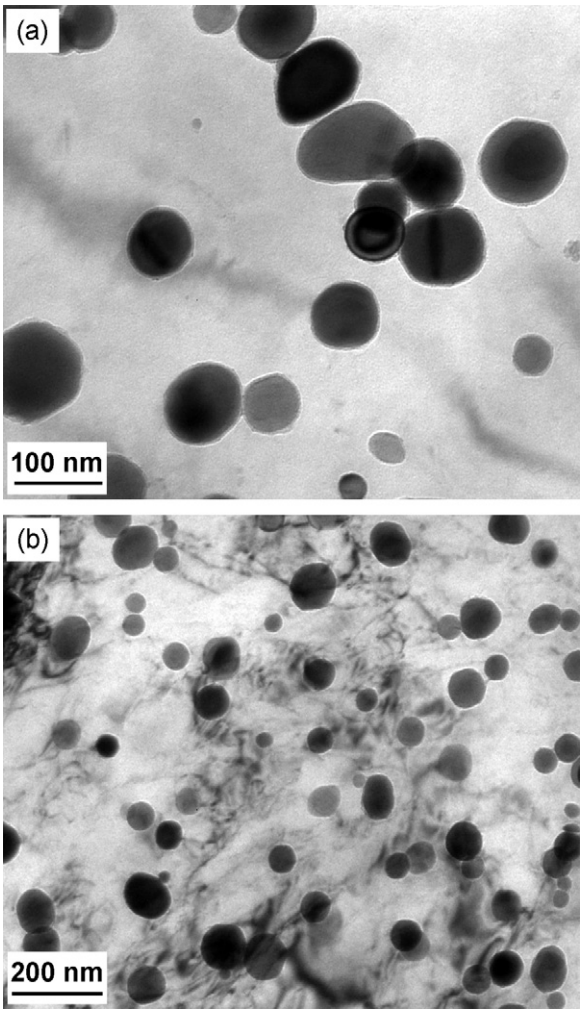


**Fig. 6.** TEM micrographs of the carbides in the specimens isothermally held at 530 °C for 3600 s without (a) and with (b) the presence of a 12-T magnetic field, respectively.

temperature. The Curie temperature is defined as the transformation point from ferromagnetic state to paramagnetic state. When a magnetic field is not applied, in the magnetization–temperature curve, the temperature at which the magnetization equals zero is defined as the Curie point. Previous works revealed that the Curie point of Fe–X alloy systems was obviously influenced by high magnetic fields [23,33]. In these Fe–X (C, B, Mo) binary systems, the Curie temperature was greatly raised by high magnetic fields. Experimental results [2] also demonstrated that the precipitation of $M_6C$ carbide was still affected by a 12-T magnetic field even at high temperatures (610 °C).

The magnetization is expressed as

$$M = NmB_j(\alpha) \tag{3}$$

where $B_j(\alpha)$ is a Brillouin function and is defined as

$$B_j(\alpha) = \left\{ \frac{2j+1}{2j} \mathrm{cth}\frac{(2j+1)a_j}{2j} - \frac{1}{2j}\mathrm{cth}\frac{a_j}{2j} \right\} \tag{4}$$

$$\alpha_j = \frac{n_B \mu_B B}{kT} \tag{5}$$

On the basis of the above equations (1)–(5), the temperature variations of magnetization for $Fe_2C$, $Fe_3C$ and $Fe_3Mo_3C$ carbides were calculated and are illustrated in Fig. 7. As a reference those of α-Fe were also calculated and displayed in the same figure. Generally, it is seen that the magnetization decreases with increasing

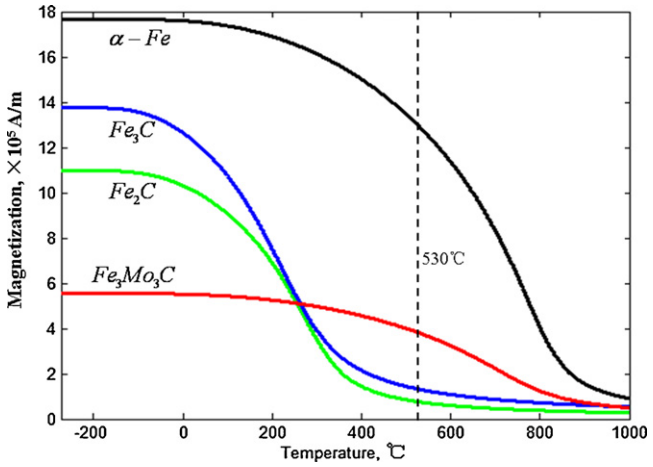


**Fig. 7.** The temperature variations of magnetization of for α-Fe and $Fe_2C$, $Fe_3C$, $Fe_3Mo_3C$ carbides. The dotted line represents the magnetization value of α-Fe and different carbides at 530 °C.

temperature. It is also seen that when the temperature reaches 530 °C (dotted line), the magnetization of $Fe_3Mo_3C$ is obviously higher than that of $Fe_2C$ and $Fe_3C$. Theoretically, the Gibbs free energy is lowered in relation to their magnetization. Therefore, in a 12-T magnetic field, the Gibbs free energy of $Fe_3Mo_3C$ drops beyond that of $Fe_2C$ and $Fe_3C$. It suggests that $Fe_3Mo_3C$ becomes more stable than $Fe_2C$ and $Fe_3C$ at this temperature. According to the $\int B_0 \cdot dM$, the relative magnetic free energy change approximates $9.08 \times 10^5$, $15.84 \times 10^5$, $45.72 \times 10^5$ J/mol under a 12-T magnetic field for three carbides $Fe_2C$, $Fe_3C$ and $Fe_3Mo_3C$, respectively. Therefore the influence of the magnetic field on the Gibbs free energy of $M_6C$ ($Fe_3Mo_3C$) is the most remarkable. As a result, the precipitation of $M_6C$ is promoted by the application of a 12-T magnetic field.

### 4.3. Influence of strong magnetic field on the concentration of Fe and Mo atoms in the carbide of $M_6C$

The total magnetic moments per unit cell of transition carbide have been obtained using first principle calculation [29,31]. The all-electron FPLAPW method was used as embodied in the WIEN2K code [34]. The exchange-correlation potential was calculated using the generalized gradient approximation (GGA) via the scheme of Perdew-Burke-Ernzerhof 96 (PBE-GGA) [35]. The electronic wave functions were sampled with 47 k and 72 k points in the irreducible Brillouin zone of $Fe_2Mo_4C$ and $Fe_3Mo_3C$, respectively. WIEN2K generates the k-mesh in the irreducible wedge of the Brillouin zone on a special point grid, which can be used in an improved tetrahedron integration scheme [36]. The sphere radii (muffin tin) were different for iron, molybdenum and carbon: $R_{MT}$ = 2.22 a.u. for iron atoms, $R_{MT}$ = 2.10 a.u. for molybdenum atoms and $R_{MT}$ = 1.86 a.u. for carbon ones. The use of the full potential ensured that the calculation was completely independent of the choice of the sphere radii. Correspondingly 2453 and 2433 plane waves were used for $Fe_2Mo_4C$ and $Fe_3Mo_3C$, respectively. Table 5 shows the magnetic moments of $Fe_2Mo_4C$ and $Fe_3Mo_3C$ per Fe atom. The calculated total magnetic moments per unit cell were 2.37 $\mu_B$, and 5.11 $\mu_B$ for $Fe_2Mo_4C$ and $Fe_3Mo_3C$, respectively. The calculated results of $M_6C$ carbides

**Table 5**
The calculated magnetic moments ($\mu_B$) of different carbides per Fe atom.

| Phases | $Fe_2Mo_4C$ | $Fe_3Mo_3C$ | |
|---|---|---|---|
| Wyckoff sites of Fe | 32e | 32e | 16d |
| Magnetic moments per Fe atom ($\mu_B$) | 1.33 | 1.86 | 1.85 |

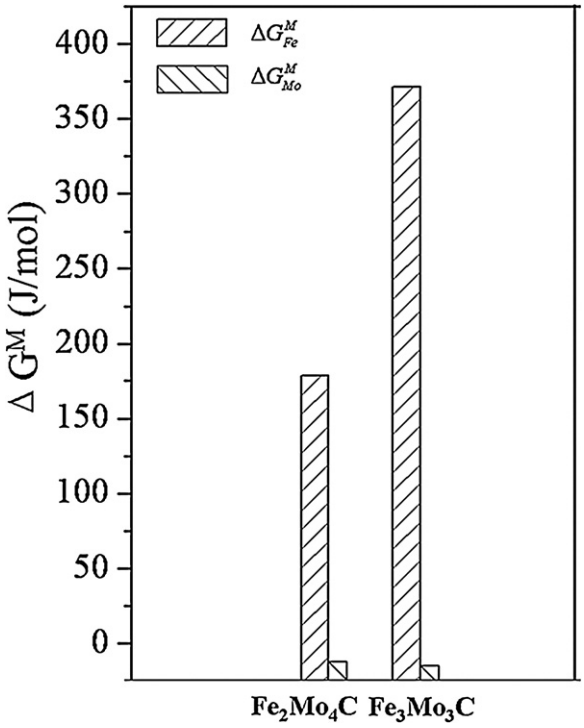


**Fig. 8.** The magnetic free energy change of Fe and Mo atoms in different type alloy carbides of $M_6C$ ($Fe_2Mo_4C$, $Fe_3Mo_3C$).

demonstrate that the magnetic moment of $Fe_2Mo_4C$ is lower than that of $Fe_3Mo_3C$ carbide.

The influence of high magnetic field on the concentration of Fe and Mo atoms in alloy carbides mainly depends on magnetic free energy change ($\Delta G^M$) of the two atoms. The $\Delta G^M$ is associated with the magnetic moment of Fe or Mo atoms in alloy carbides. In the calculation of $Fe_2Mo_4C$, the Fe atom magnetic moment in 32e is 1.33 $\mu_B$. The locally different Fe moments are 1.86 $\mu_B$ and 1.82 $\mu_B$ at the 32e and 16d sites in $Fe_3Mo_3C$ carbide, respectively (Table 5). Given the Bohr magneton ($\mu_B = 9.3 \times 10^{-24}$ J/T), after converting to J/mol using Avogadro's number and multiplying by the magnetic moment per Fe atom, the reduction of magnetic free energy of the Fe atoms ($\Delta G^M_{Fe}$) in $Fe_2Mo_4C$, $Fe_3Mo_3C$ is 178.70 and 371.51 J/mol under a 12-T magnetic field, respectively, as shown in Fig. 8. This suggests that the increase in the concentration of Fe in the carbide can greatly lower the chemical potential of the carbide. In contrast, because of the paramagnetism of Mo atom, the magnetic free energy ($\Delta G^M_{Mo}$) of Mo atom has almostly unchanged. The magnetic field has negligible influence on free energy of the Mo atoms. The measured concentration of Fe and Mo atoms in the alloy carbide of $(Fe,Mo)_6C$ is inter-dependent. Therefore, it is evident that the measured variation tendency of concentration (Table 3) of Fe and Mo atoms in $M_6C$ carbides is consistent with the calculated relative free energy change.

## 5. Conclusions

The effect of a 12-T high magnetic field on alloy carbide precipitation in an Fe–C–Mo alloy during isothermal transformation at 530 °C for various times was studied, which leads to the following results.

(1) Three kinds of carbides ($M_2C$, $M_3C$ and $M_6C$) were precipitated in an Fe–0.28%C–3.0%Mo alloy. They are identified to be $(Fe,Mo)_2C$, $(Fe,Mo)_3C$ and $(Fe,Mo)_6C$.

(2) $(Fe,Mo)_2C$ and $(Fe,Mo)_3C$ were precipitated at earlier transformation stage and $(Fe,Mo)_6C$ was precipitated at later transformation stage when a 12-T magnetic field was not applied, whereas $(Fe,Mo)_6C$ was precipitated at all transformation stages when a 12-T magnetic field was applied. This indicates that the precipitation of $M_6C$ carbides is greatly promoted by applying high magnetic field, which is attributed to the remarkable reduction of the magnetic Gibbs free energy of $M_6C$ carbides.

(3) The concentration of substitutional solute atoms Fe and Mo in the carbide of $(Fe,Mo)_6C$ was influenced by high magnetic field. The change of concentration of substitutional solute atoms Fe and Mo was caused by their differences in magnetic moments.

## Acknowledgments

The authors are grateful to Professor M. Enomoto, Ibaraki University, Japan, for providing alloy specimens. The authors are also grateful to the financial support for this work from State Ministry of Education (Grant No. NCET-05-0680), Natural Science Foundation of Hubei Province (Grant No. 2006ABB037), Hubei Provincial Department of Education (Grant No. 200711001) and Hubei Province Key Laboratory for Systems Science on Metallurgical Processing (Grant No. Y201104). Thanks are also expressed for Mr. Ge He for his help to calculate Fig. 7.

## References

[1] T. Kushida, N. Kuratomi, T. Kudoh, H. Matsumoto, T. Tsumura, F. Nakasato, Tetsu-to-Hagane 82 (1996) 297.
[2] Z.N. Zhou, K.M. Wu, Scripta Mater. 61 (2009) 670.
[3] H. Tsubakino, H.I. Aaronson, Metall. Trans. 18A (1987) 2047.
[4] W.T. Reynolds, F.Z. Li, C.K. Shui, H.I. Aaronson, Metall. Trans. 21A (1990) 1433.
[5] K.M. Wu, M. Enomoto, Scripta Mater. 46 (2002) 569.
[6] K.M. Wu, M. Kagayama, M. Enomoto, Mater. Sci. Eng. 343A (2003) 143.
[7] M. Enomoto, N. Maruyama, K.M. Wu, T. Tarui, Mater. Sci. Eng. 343A (2003) 151.
[8] M. Enomoto, K.M. Wu, M. Kagayama, CAMP-ISIJ 17 (2004) 1223.
[9] D.V. Shtansky, G. Inden, Acta Mater. 45 (1997) 2861.
[10] R.C. Thomson, M.K. Miller, Acta Mater. 46 (1998) 2203.
[11] A. Vyrostkova, A. Kroupa, J. Janovec, M. Svoboda, Acta Mater. 46 (1998) 31.
[12] A. Kroupa, A. Vyrostkova, M. Svoboda, J. Janovec, Acta Mater. 46 (1998) 39.
[13] Y.D. Zhang, N. Gey, C.S. He, X. Zhao, L. Zuo, C. Esling, Acta Mater. 52 (2004) 3467.
[14] Y.D. Zhang, X. Zhao, N. Bozzolo, C. He, L. Zuo, C. Esling, ISIJ Int. 45 (2005) 913.
[15] T. Kakeshita, K. Kuroiwa, K. Shimizu, T. Ikeda, A. Yamagishi, M. Date, Mater. Trans. 34 (1993) 423.
[16] H. Ohtsuka, X.J. Hao, H. Wada, Mater. Trans. 44 (2003) 2529.
[17] H. Ohtsuka, Curr. Opin. Solid State. Mater. Sci. 8 (2004) 279.
[18] H. Ohtsuka, Mater. Sci. Eng. 438A (2006) 136.
[19] M. Enomoto, H. Guo, Y. Tazuke, Y.R. Abe, M. Shimotomai, Metall. Mater. Trans. 32A (2001) 445.
[20] G.M. Ludtka, R.A. Jaramillo, R.A. Kisner, D.M. Nicholson, J.B. Wilgen, G. Mackiewicz-Ludtka, P.N. Kalu, Scripta. Mater. 51 (2004) 171.
[21] G.H. Zhang, M. Enomoto, Mater. Sci. Technol. 26 (2010) 269.
[22] D.A. Molodov, P.J. Konijnenburg, Scripta. Mater. 54 (2006) 977.
[23] X.J. Liu, Y.M. Fang, C.P. Wang, Y.Q. Ma, D.L. Peng, J. Alloys Compd. 459 (2008) 169.
[24] A.T. Davenport, R.W.K. Honeycombe, Met. Sci. 9 (1975) 201.
[25] T. Sato, T. Nishizawa, K. Tamaki, Trans. JIM 3 (1962) 196.
[26] B. Uhrenius, H. Harvig, Met. Sci. 9 (2) (1975) 67.
[27] L.R. Woodyatt, G. Krauss, Metall. Mater. Trans. A 10A (1979) 1893.
[28] T. Takei, Kinzoku. No. Kenkyu 9 (1932) 97.
[29] T.P. Hou, Y. Li, J.J. Zhang, K.M. Wu, J. Magn. Magn. Mater. 324 (2012) 857.
[30] E. Du Trémolet de Lacheisserie, Magnétisme-Fondements, vol. 1, Grenoble Sciences, Grenoble, 2000, p. 68.
[31] H. Faraoun, Y.D. Zhang, C. Esling, H. Aourag, J. Appl. Phys. 99 (2006), 093508-1.
[32] B.D. Cullity, Introduction to Magnetic Materials, Addison-Wesley, Reading, MA, 1972, pp. 117–155.
[33] H. Guo, M. Enomoto, Mater. Trans. JIM 41 (2000) 911.
[34] P. Blaha, K. Schwarz, G.K.H. Madsen, D. Kvasnicka, J. Luitz, WIEN2K, an augmented plane wave + local orbital program for calculating crystal properties, Karlheinz Schwarz, Technical University at Wien, 2001.
[35] J.P. Perdew, S. Burke, M. Ernzerhof, Phys. Rev. Lett. 77 (1996) 3865.
[36] P.E. Blöchl, O. Jepsen, O.K. Andersen, Phys. Rev. B 49 (1994) 16223.